

3-2-6 New Observational Deployments for SEALION —Airglow Measurements Using All-Sky Imagers

KUBOTA Minoru, ISHII Mamoru, TSUGAWA Takuya, UEMOTO Jyunpei,
JIN Hidekatsu, OTSUKA Yuichi, and SHIOKAWA Kazuo

An airglow all-sky imager (ASI)—a new monitoring instrument—is scheduled to be set up in February 2010 at Chiang Mai, Thailand, as part of the framework of the Southeast Asia Low-latitude Ionospheric Network (SEALION) being developed in the Southeast Asian region by the National Institute of Information and Communications Technology (NICT). The ASI images airglow having an emission layer near the ionospheric F-layer in order to observe the two-dimensional structure and time evolution of such ionospheric disturbances as plasma bubbles. In Southeast Asia, the Solar-Terrestrial Environment Laboratory (STE) of Nagoya University has been conducting ASI-based observations at Kototabang, Indonesia, ever since 2002. This paper provides detailed insight into the formation, growth and propagation of plasma bubbles as derived from observational data recorded using ASI at Kototabang and using SEALION ionosondes and GPS receivers. The functional requirements for another ASI to be installed and ASI-based observation schemes are then discussed based on that insight.

Keywords

Airglow, Ionosphere, Plasma bubble, Gravity wave

1 Introduction

When an image of airglow with OI 630.0 nm is taken in the equatorial anomaly region, the phenomenon-like black shadows of airglow are observed in some cases as shown in Fig. 1. These black shadows (with significantly decreased airglow emission intensity) often drift eastward and branch out like the

branches of a tree, with each branch being about 100-km wide. This phenomenon is induced by a plasma bubble, as discussed in this feature edition [1][2] and often observed in Japan as well during an active solar activity period.

Plasma bubbles have been observed using airglow all-sky imagers (ASIs) since the 1980s (see [3] and other references). ASI-

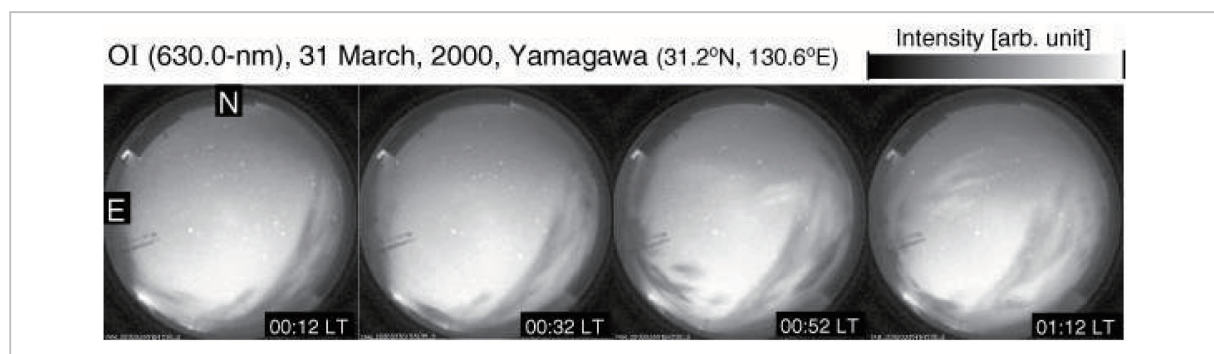


Fig. 1 Plasma bubble observed at Yamagawa Observatory

based observations reveal the geometry of a plasma bubble, its drift velocity, and how it grows. Recent advances in optics have driven research to observe the microstructures and growth process of plasma bubbles, and probe into their relation with plasma instability [4][5]. Reference [6] reports that the simultaneous observations of plasma bubbles at geomagnetic conjugate points from Sata, Japan, and Darwin, Australia, had confirmed the precise conjugacy in place between plasma bubbles in the Northern and Southern Hemispheres.

Electron density decreases within a plasma bubble. It is accompanied by the growth of ionospheric irregularities with various scales [7]. Positioning satellite radio waves passing through plasma bubbles are subject to scintillation, resulting in degraded positioning accuracy or sometimes poor reception. The construction of SEALION is intended to establish technology for predicting the occurrence and arrival of plasma bubbles that could have a major impact on satellite positioning.

Past studies have revealed the seasonal dependence and solar activity dependence on the occurrence frequency of plasma bubbles [8]. However, the causes of day-to-day variations in the occurrence of plasma bubbles have yet to be identified. Plasma bubbles form in the vicinity of the magnetic equator, with some growing toward a higher-latitude region, and others not. The reasons for this difference have also not been discussed in depth. These mechanisms must therefore be explored in order to make a major step toward the forecasting of plasma bubbles.

Some previous reports have also suggested the involvement of large-scale atmospheric waves spanning an east-west wavelength of several hundred kilometers in the mechanism of plasma bubble occurrence [9][10]. The ASI should be able to capture any such large-scale atmospheric waves existing at the ionospheric F-layer height. This paper introduces the principles of ASI-based ionospheric observation, presents detailed pictures of plasma bubbles provided by the ASI, and discusses the possibilities and planning of ASI-based, large-scale

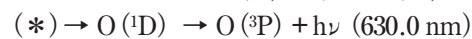
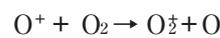
atmospheric wave observations.

2 Principles of ASI-based observation and overview of equipment

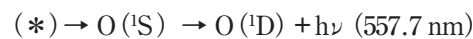
2.1 Principles of airglow-based ionospheric observation

Typical airglows used in ionospheric observations from the ground are OI 630.0, 557.7 and 777.4 nm. The mechanism of airglow excitation (as reported in [10] to [13]) is expressed in the following reaction formulas:

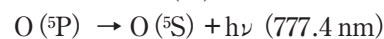
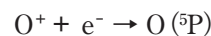
OI630.0 nm :



OI557.7 nm :



OI777.4 nm :



As can be seen from these reaction formulas, the excitation of airglow with OI 630.0 and 557.7 nm is governed by the collision reaction between O^+ (i.e., main component ion of the ionospheric F-region) and oxygen molecules (i.e., neutral atmosphere). The excitation of airglow with OI 777.4 nm is governed by the collision reaction between O^+ and electrons. Figure 2 schematically shows such dif-

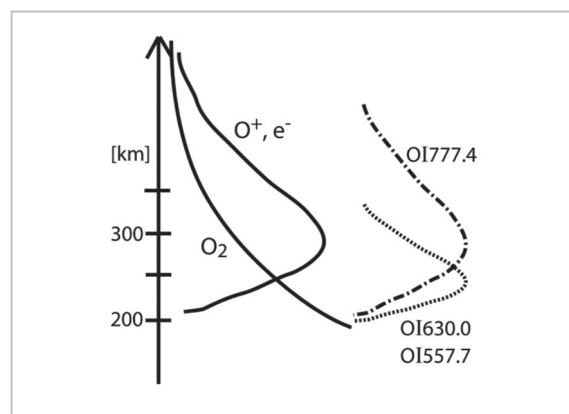


Fig.2 Schematic view of height distributions of O^+ , electrons and oxygen molecules, and profile of airglow emission height

ferences in excitation reaction manifested as differences in the light-emitting height. This means that airglow with OI 630.0 and 557.7 nm have emissions peaking about 50 km below the peak height of the F-region, as compared to airglow with OI 777.4 nm emitting most intensely near the peak height of the F-region. Thus, using these emissions makes it possible to collect information about two different heights of the ionosphere.

When a plasma bubble forms in the ionosphere, prevailing O^+ and electrons will sharply decrease. Consequently, the airglow emission intensity is degraded and airglow is observed like a black shadow as shown in Fig. 1. Conversely, variations in ionospheric electron density can be determined from changes in emission intensity. However, the relation between variations in ionospheric electron density and airglow emission intensity should be interpreted with discretion [14]. Because the airglow emission intensity also depends on the changes in the ionospheric F-layer height, and airglow with OI 557.7 nm is emitted even at a height of about 95 km with another excitation mechanism.

2.2 Overview of ASI equipment

The ASI unit employs a fish-eye objective lens to monitor an all-sky visual field of 180 degrees, making it possible to capture in a single view the entire range centering on an observation point several hundred kilometers

in diameter. Light leaving the objective lens is converted through a telecentric lens into parallel rays that are separated via an interference filter before focusing within the photodetector. The interference filter is mounted on five to six selectable channels of filter turrets to allow observation on multiple wavelengths. A cooled CCD camera with a back-illuminated CCD device is used as the photodetector for higher sensitivity and easier handling. Such observation procedures as opening and closing the shutter, changing filters, and imaging and saving data are performed by a program running on an ASI control PC. The program proceeds with sequential imaging by switching the channels as scheduled. Figure 3 shows sample observations of two kinds of airglow and background light imaged by a single ASI virtually at the same time (with a time difference of up to five minutes).

In this diagram, all-sky images of airglow with OI 630.0 nm, airglow with OI 557.7 nm, and background light are arranged from left to right. A totally different phenomenon appears in each image. The image of airglow with OI 630.0 nm is found to have a plasma bubble forming on the southwestern side. Conversely, the image of airglow with OI 557.7 nm does not exhibit an evident plasma bubble, but instead shows a light wave structure from the zenith to the eastern side. Such a pattern is characteristic of atmospheric gravity waves at the E-layer height. Neither a plasma bubble

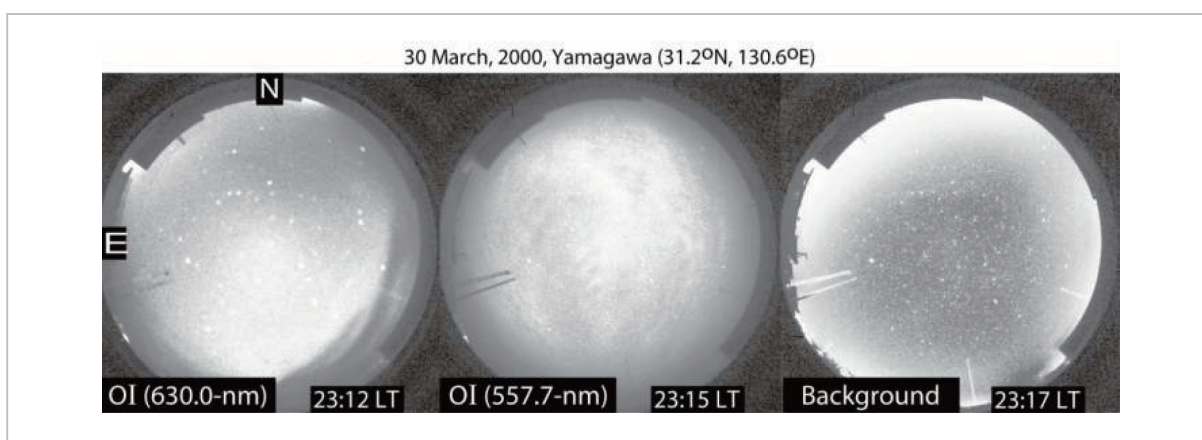


Fig.3 Two kinds of airglow observed at Yamagawa Observatory, and all-sky image of background light

structure nor a wave structure is found on the background light channel, where only multiple stars are mapped. This finding supports conjecture that the structures mapped in the first two images were not caused by clouds.

NICT has developed an ASI powered by a wavelength-specific focus adjustment feature [15]. It has also established a technique by which to derive the absolute intensity of airglow from calibration data available from the National Institute of Polar Research [17]. Plans call for NICT's ASI to be set up in February 2010 at Sirindhorn Observatory (18.8° N latitude, 98.9° E longitude, 13° dip latitude) in Chiang Mai, Thailand, in order to launch a steady observation program, jointly with the University of Chiang Mai and the Solar-Terrestrial Environment Laboratory (STE) of Nagoya University.

3 Preliminary survey using the Kototabang ASI

In the Southeast Asian region, the ASI [18][19] set up by STE was commissioned into service in 2002 at Kototabang, Indonesia (0.2° S latitude, 100.3° E longitude, -10° dip latitude), and has already accumulated six years' worth of data. There is a roughly magnetic conjugate relation between Kototabang and Chiang Mai. Prominent plasma bubble events obtained by surveying the data obtained at those locations were subjected to integrated analysis, together with other observational data from SEALION.

Figure 4 shows the variations in airglow with OI 630.0 nm on January 29, 2006, as observed by the ASI in Kototabang. The figure gives imaging data virtually six minutes apart from 14:30 UT (21:30 LT) to 15:45 UT (22:45 LT).

Each panel takes the deviation from hourly averages of airglow intensity to enhance airglow variations for mapping centered on Kototabang. A plasma bubble appeared somewhat eastward above Kototabang a little before 21:30 LT and structurally drifted eastward, while subsequently expanding the dis-

turbed region westward. An eastward drift velocity of about 110 m/s can be read from this diagram. This value matches the plasma bubble drift velocity obtained from satellites or GPS scintillation observations reported to date ([20]-[22] and other references). This plasma bubble then shrank at around 15:00 UT (24:00 LT), but was continuously observed until around 22:00 UT (05:00 LT) before dawn.

Figure 5 is an example of the SEALION integrated analysis panel in which SEALION ionograms and GPS-TECs in effect at 16:00 UT (23:00 LT) amid a plasma bubble are tiled.

Summary descriptions of the SEALION observation points and observation equipment can be found in Reference [1]. In addition to the Kototabang ASI run by the STE, ionosonde observations were also conducted at Chumphon (Thailand), Kototabang, and Bac Lieu (Vietnam) on that day, along with GPS-TEC observations at Chiang Mai, Chumphon, and Kototabang. As can be seen in Fig. 5, all ionograms recorded at the three locations demonstrated the spread-F state, with GPS-ROTI on the increase. (Pink lines in the summary ionogram and the GPS-TEC&ROTI panel denote the current time of 16:00 UT (23:00 LT). Time-dependent changes in the ionospheric F-layer height visible in the summary ionogram apparently suggest that the height is falling at Chumphon but virtually bottomed out at Kototabang at 16:00 UT (23:00 LT).

We have created an analysis tool capable of tracking time-dependent changes in observational data for display in an animated view, and used the tool to analyze events in detail. Figure 6 gives a summary view of the progress of plasma bubble events occurred in that evening.

As in apparent in Fig. 6, a sequence of plasma bubble events gives different looks (such as regarding the phenomenon's duration) depending on the kind of equipment used to observe the events. A detailed discussion of the differences in how the plasma bubble events look depending on the kind of equip-

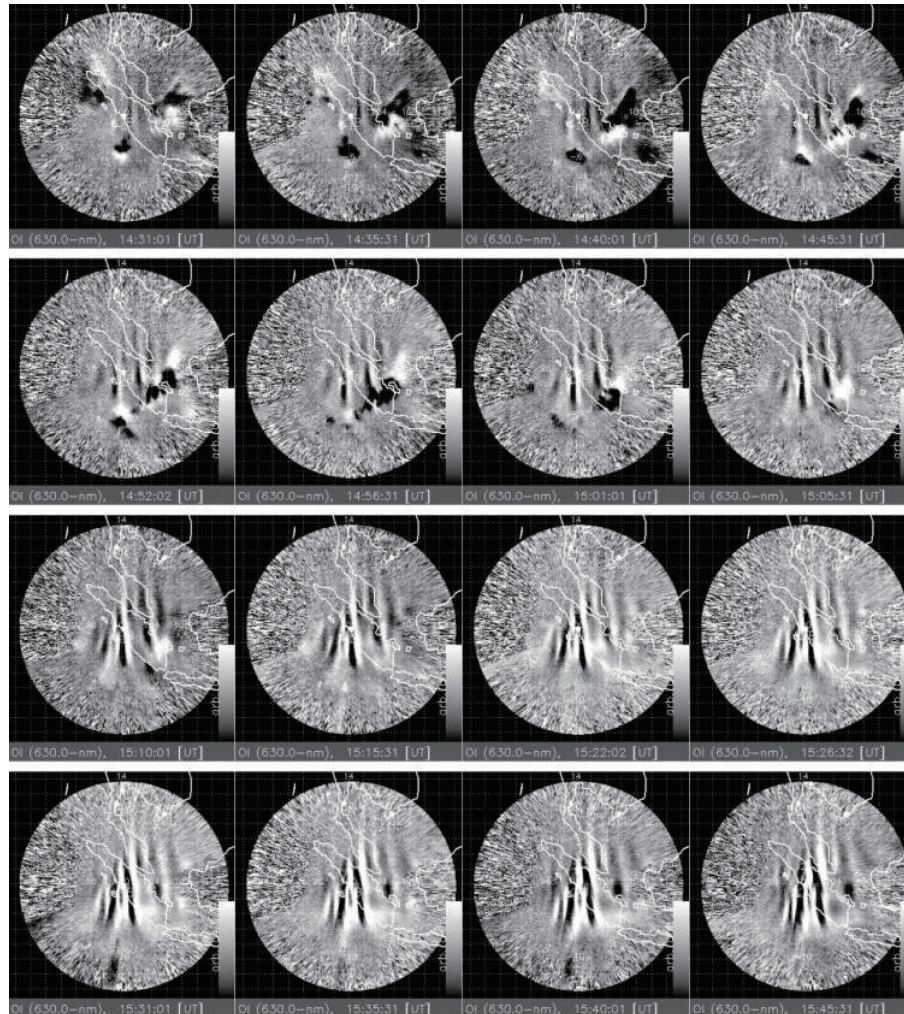


Fig.4 Sample observations of a plasma bubble by the ASI set up in Kototabang (on January 29, 2006)

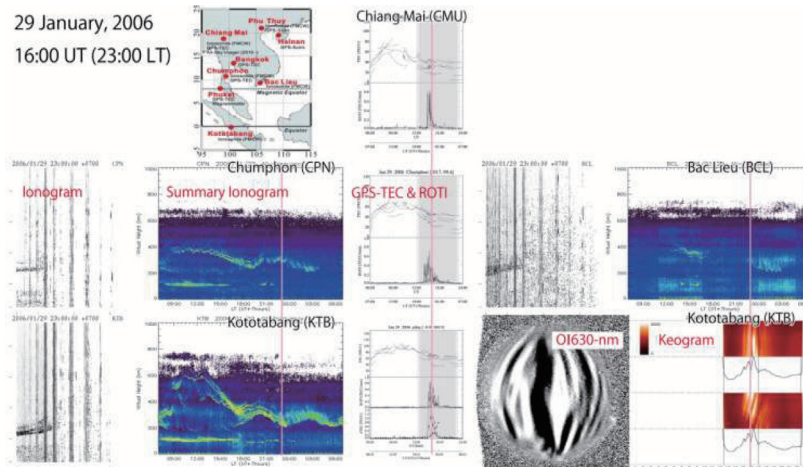


Fig.5 SEALION integrated analysis panel at 16:00 UT on January 29, 2006

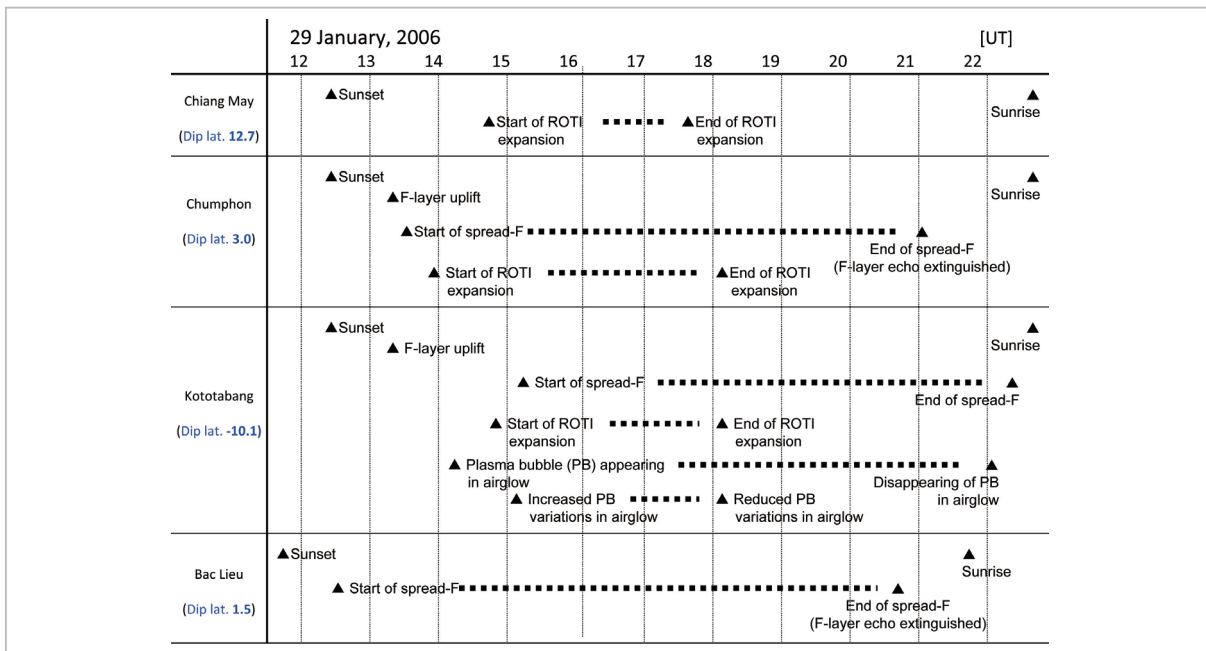


Fig.6 Progress of plasma bubble events observed on January 29, 2006

ment used is beyond the scope of this paper.

4 ASI installation in Chiang Mai, Thailand, and its observation targets

As can be seen from these sample observations, the ASI is a unique observation instrument that sensitively captures plasma bubbles upon occurrence, and monitors the growth and propagation of these formations in detail. However, its major drawback is that the chances for observation depend on weather and moon-lighting conditions. The geographic location of Kototabang in the climatic division of a tropical rainforest affords few clear-sky days year-round, and only 62 nights during a six-year period (covering about 2,200 nights) allowed clear-sky observation for an uninterrupted period of at least six hours.

As stated earlier, we expect to set up a new ASI at Sirindhorn Observatory (18.8° N latitude, 98.9° E longitude, 13° dip latitude) in Chiang Mai, Thailand, which has a magnetic conjugate relation with Kototabang. Chiang Mai sits in the climatic division of a tropical savanna climate and offers the promise of far

more days of observation.

The new ASI at Sirindhorn Observatory will essentially be in daily operation, except during full-moon periods (each accounting for a total of 10 days before and after a full moon) after being set up in position in February 2010. It will monitor the following five kinds of wavelength, capturing each in a time integral of 15 seconds to about two minutes:

- OI 630.0 nm ... Observation of the ionospheric F-layer bottomside
- OI 777.4 nm ... Observation near the peak in the ionospheric F-layer
- OH Meinel band ... Observation of atmospheric gravity waves in the vicinity of mesopause (at an approximate height of 86 km)
- Sodium D-line ... Observation of atmospheric gravity waves in the vicinity of mesopause (at an approximate height of 92 km)
- Background light (572.3 nm)

Observations will be conducted with time resolutions (imaging intervals) of about six minutes (and three minutes only in the OH Meinel band). Summary observational data will be transferred to NICT in Japan via a net-

work, with bulky raw data being mailed to Japan. NICT expects to work out a processing program for the summary data and will publicize the observation times, observed wavelengths, clear-sky status, and summary data on the SEALION website or elsewhere.

We intend to leverage the new ASI to detect large-scale atmospheric waves, as well as ionospheric disturbances. Atmospheric waves that contribute to the occurrence of plasma bubbles have an east-west wavelength of about 800 km as suggested in References [9] and [10]. The ASI makes it possible to observe a full visual field at least 800 km in diameter in the planetary scale mesopause region (up to 100 km in height) or a region at least 1500 km in diameter at ionospheric height, all in a single view. Given its wide visual field reach, the ASI can fully observe the large-scale atmospheric waves of a specific target.

In addition to its extensive visual field reach, the ASI can obtain fine-quality airglow images along with stellar images, the Milky Way, background light, and other elements properly corrected as necessary to observe large-scale atmospheric waves. This is because the quality of such correction processing has significant bearing on the analytical accuracy of two-dimensional FFT and other manipulations needed to spot large-scale atmospheric waves. Stars appearing as sharp as possible are useful for removing stellar images. In this regard, the focus adjustment feature of the new ASI should prove very beneficial.

Of the five channels mentioned above, the OH Meinel band and the sodium D-line are suited for observing atmospheric gravity waves in the mesopause. According to Reference [23], atmospheric gravity waves propagating through this region with a horizontal wavelength of about 700 km had been detect-

ed from ASI-based observational data on airglow obtained in Kagoshima, Japan, thereby attesting to the applicability of this method for detecting large-scale atmospheric waves in a low-latitude region as well. In the meantime, F-layer region information is derived from observing airglow with OI 630.0 and 777.4 nm. Such airglow is superimposed with two kinds of airglow intensity variations: one originating from ionospheric disturbances such as plasma bubbles, and one originating from the neutral atmosphere. Any large-scale atmospheric waves in the F-region that are spotted in ASI-based observational data should significantly help to elucidate the mechanism of plasma bubble occurrence.

5 Conclusions

An airglow all-sky imager (ASI) scheduled to be set up in February 2010 at Sirindhorn Observatory in Chiang Mai, Thailand (as part of SEALION) has been discussed regarding the following points:

- The principles of ASI-based observation have been introduced and sample observations reviewed to point out the advantages of using the ASI in conjunction with ionosondes and GPS receivers, in order to gain detailed features of plasma bubbles.
- Specifications of the new ASI to be set up in Chiang Mai, Thailand have been summarized, along with relevant observation plans and possible benefits.
- We have stated that ASI-based observations are geared toward a key target of detecting large-scale atmospheric waves—a probable factor contributing to the mechanism of plasma bubble occurrence—and demonstrated that ASI offers the observational accuracy necessary for this task.

References

- 1 T. Maruyama, S. Saito, M. Kawamura, K. Nozaki, J. Uemoto, T. Tsugawa, H. Jin, M. Ishii, and M. Kubota, "Outline of the SEALION Project and Initial Results," Special issue of this NICT Journal, 3-2-1, 2009.

- 2 S. Saito, T. Maruyama, M. Ishii, and M. Kubota, "Observations of Plasma Bubbles by HF-TEP and GPS Scintillation," Special issue of this NICT Journal, 3-2-8, 2009.
- 3 M. Mendillo and A. Tyler, "Geometry of depleted plasma regions in the equatorial ionosphere," *J. Geophys. Res.*, 88 (A7), 5778–5782, 1983.
- 4 J. J. Makela, M. C. Kelley, and M. J. Nicolls, "Optical observations of the development of secondary instabilities on the eastern wall of an equatorial plasma bubble," *J. Geophys. Res.*, Vol. 111, A09311, doi: 10.1029/2006JA011646, 2006.
- 5 J. J. Makela and E. S. Miller, "Optical observations of the growth and day-to-day variability of equatorial plasma bubbles," *J. Geophys. Res.*, Vol. 113, A03307, doi: 10.1029/2007JA012661, 2008.
- 6 Y. Otsuka, K. Shiokawa, T. Ogawa, and P. Wilkinson, "Geomagnetic conjugate observations of equatorial airglow depletions," *Geophys. Res. Lett.*, 29 (15), 1753, doi: 10.1029/2002GL015347, 2002.
- 7 Y. Otsuka, K. Shiokawa, T. Ogawa, T. Yokoyama, M. Yamamoto, and S. Fukao, "Spatial relationship of equatorial plasma bubbles and field-aligned irregularities observed with an allsky airglow imager and the Equatorial Atmosphere Radar," *Geophys. Res. Lett.*, 31, L20802, 10.1029/2004GL020869, 2004.
- 8 M. Nishioka, A. Saito, and T. Tsugawa, "Occurrence characteristics of plasma bubble derived from global ground-based GPS receiver networks," *J. Geophys. Res.*, Vol. 113, A05301, doi: 10.1029/2007JA012605, 2008.
- 9 Roland T. Tsunoda, "On the enigma of day-to-day variability in equatorial spread F," *Geophys. Res. Lett.*, Vol. 32, L08103, doi: 10.1029/2005GL022512, 2005.
- 10 Smitha V. Thampi, Mamoru Yamamoto, Roland T. Tsunoda, Yuichi Otsuka, Takuya Tsugawa, Jyunpei Uemoto, and Mamoru Ishii, "First observations of large-scale wave structure and equatorial spread F using CERTO radio beacon on the C/NOFS satellite," *Geophys. Res. Lett.*, Vol. 36, L18111, doi: 10.1029/2009GL039887, 2009.
- 11 B. A. Tinsley and J. A. Bittencourt, "Determination of F region height and peak electron density at night using airglow emissions from atomic oxygen," *J. Geophys. Res.*, 80 (16), 2333–2337, 1975.
- 12 B. A. Tinsley, A. B. Christensen, J. Bittencourt, H. Gouveia, P. D. Angreji, and H. Takahashi, "Excitation of oxygen permitted line emissions in the tropical nightglow," *J. Geophys. Res.*, 78 (7), 1174–1186, 1973.
- 13 R. Link and L. L. Cogger, "A reexamination of the O I 6300AA nightglow," *J. Geophys. Res.*, 93 (A9), 9883–9892, 1988.
- 14 M. Kubota, H. Fukunishi, and S. Okano, "Characteristics of medium- and large-scale TIDs over Japan derived from OI 630-nm nightglow observation," *Earth Planets Space*, 53, 741–751, 2001.
- 15 M. Kubota, M. Ishii, S-I. Oyama, and Y. Murayama, "Recent results and future plans of atmospheric study using CRL all-sky imagers," *Journal of the Communications Research Laboratory*, 49, 161–171, June 2002.
- 16 S. Okano, S. Takeshita, and M. Taguchi, "Absolute calibration system at NIPR for aurora/ airglow measurements using a 1.9-m integration sphere," *Proc. 24th Annual European Meeting on Atmospheric Studies by Optical Method*, 30, 333, 1998.
- 17 M. Yamamoto, M. Kubota, S. Takeshita, M. Ishii, Y. Murayama, and M. Ejiri, "Calibration of CRL all-sky imagers using an integrating sphere," *Advances in Polar Upper Atmosphere Research*, 16, 173–180, Sep, 2002.
- 18 K. Shiokawa, Y. Katoh, M. Satoh, M. Ejiri, T. Ogawa, T. Nakamura, T. Tsuda, and R. H. Wiens, "Development of optical mesosphere thermosphere imagers (OMTI)," *Earth Planets Space*, 51, 887–896, 1999.

- 19 K. Shiokawa, Y. Otsuka, and T. Ogawa, "Propagation characteristics of nighttime mesospheric and thermospheric waves observed by optical mesosphere thermosphere imagers at middle and low latitudes," *Earth Planets Space*, 61, 479–491, 2009.
- 20 T. Ogawa, E. Sagawa, Y. Otsuka, K. Shiokawa, T. I. Immel, S. B. Mende, and P. Wilkinson, "Simultaneous ground-and satellite-based airglow observations of geomagnetic conjugate plasma bubbles in the equatorial anomaly," *Earth Planets Space*, 57, 385–392, 2005.
- 21 Y. Otsuka, K. Shiokawa, and T. Ogawa, "Equatorial Ionospheric Scintillations and Zonal Irregularity Drifts Observed with Closely-Spaced GPS Receivers in Indonesia," *Journal of the Meteorological Society of Japan*, Vol. 84A, pp. 343–351, 2006.
- 22 S. Saito, T. Maruyama, M. Ishii, M. Kubota, G. Ma, Y. Chen, J. Li, C. H. Duyen, and T. L. Truong, "Observations of small- to large-scale ionospheric irregularities associated with plasma bubbles with a transequatorial HF propagation experiment and spaced GPS receivers," *J. Geophys. Res.*, Vol. 113, A12313, doi: 10.1029/2008JA013149, 2008.
- 23 M. Kubota, S. Kawamura, M. Abo, Y. Koizumi, Y. Murayama, M. Yamamori, K. Shiokawa, Y. Otsuka, M. Uchiumi, K. Igarashi, T. Abe, K.-I. Oyama, and N. Iwagami, "A fast-propagating, large-scale atmospheric gravity wave observed in the WAVE2004 campaign," *J. Geophys. Res.*, Vol. 111, Issue: D21, Article No. D21110, 2006.



KUBOTA Minoru, Ph.D.
Senior Researcher, Space Environment
Group, Applied Electromagnetic
Research Center
Aeronomy

ISHII Mamoru, Dr. Sci.
Director, Project Promotion Office,
Applied Electromagnetic Research
Center
Upper Atmospheric Physics



TSUGAWA Takuya, Ph.D.
Expert Researcher, Space Environment
Group, Applied Electromagnetic
Research Center
Upper Atmosphere Physics

UEMOTO Jyunpei, Ph.D.
Expert Researcher, Space Environment
Group, Applied Electromagnetic
Research Center
Aeronomy



JIN Hidekatsu, Dr. Sci.
Expert Researcher, Space Environment
Group, Applied Electromagnetic
Research Center
Upper Atmospheric Physics

OTSUKA Yuichi, Ph.D.
Assistant Professor, Solar-Terrestrial
Environment Laboratory, Nagoya
University
Aeronomy



SHIOKAWA Kazuo, Ph.D.
Professor, The Solar-Terrestrial
Environment Laboratory, Nagoya
University
Aeronomy